

Jets in Deep Inelastic Scattering and High Energy Photoproduction at HERA *

Gerd W. Buschhorn
Max-Planck-Institut für Physik
(Werner-Heisenberg-Institut)
Föhringer Ring 6
80805 München

Abstract

Recent results on jet production in neutral current deep inelastic scattering and high energy photoproduction at the HERA electron-proton-collider are briefly reviewed. The results are compared to QCD expectations in NLO and α_s determinations using these data are summarized.

1 Introduction

The hard partonic interactions at the center of photon-induced hadronic processes in deep inelastic electron/positron-proton-scattering are characterised by jets. The virtuality Q^2 of the exchanged photon can be varied from high values in deep inelastic scattering (DIS) to zero in photoproduction. According to the factorization theorem the hadronic process can be factorized into a perturbatively treated hard part, which includes the evolution of the parton entering the hard process, and a soft part, which describes the parton distribution of the target nucleon; the characteristic energy for this separation is given by the factorization scale. In DIS processes involving light quarks only, an energy scale is provided by Q^2 or the transverse energy of the emerging hadronic jet (or jet system), whereas in photoproduction the jet energy is the only available energy scale; in heavy quark production the quark mass may provide an additional energy scale. In jet studies details of the hard QCD calculations and their matching to the evolution of the target partons are probed; the investigations may also provide information on the parton distribution functions (pdfs) of the proton and photon and can serve to measure α_s and its scale dependence.

In this report, recent results from the H1- and ZEUS-collaboration on the production of standard jets i.e. jets without heavy quark tagging in neutral current DIS processes and photoproduction are discussed; jets from diffractive processes and jet shapes are not included.

*Talk given at the 9th Adriatic Meeting “Particle Physics and the Universe” in Dubrovnik/Croatia, 4.-24. September 2003

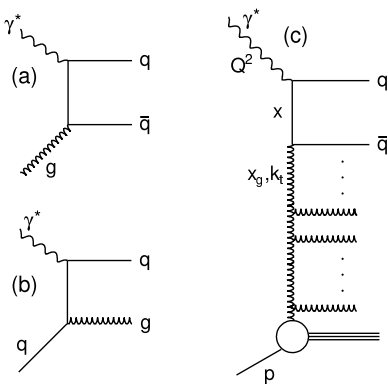


Figure 1: Leading order diagrams for jet production in photon-proton-interaction: (a) photon-gluon-fusion; (b) QCD-Compton process; (c) parton evolution

For jet studies in DIS the Breit frame is preferred, which in the quark parton model (QPM) is defined as the reference frame in which the struck parton emerges collinear with the incoming purely time-like virtual photon $\mathbf{q} = (0, 0, -Q)$ such that $2x\mathbf{p} + \mathbf{q} = 0$. Working in the Breit frame suppresses the QPM background and provides maximum separation between fragments from hard scattering QCD processes and beam remnants. Since the Breit frame is related to the photon-hadron-cms by a boost in proton beam direction (defined as $+z$ -direction), jet variables are convenient, which are boost-invariant - like the transverse energy E_T , the azimuthal angle ϕ and the pseudorapidity $\eta = -\ln \tan(\theta/2)$.

The jet finding algorithm has to be stable against infrared radiation and collinear splitting and has to take into account the fact that at HERA not all final state particles are detected. In recent years, the algorithm preferred in jet studies by the HERA-collaborations has become the inclusive k_T -cluster algorithm [1]. The algorithm proceeds by calculating for each track or energy cluster i the quantity $d_i = (E_{Ti})^2$ and for each pair i, j the quantity $d_{ij} = \min(E_{Ti}^2, E_{Tj}^2)[(\eta_i - \eta_j)^2 + (\phi_i - \phi_j)^2]$. If of all resulting $\{d_i, d_{ij}\}$ the smallest one belongs to $\{d_i\}$ it is kept as a jet and not treated further, if it belongs to $\{d_{ij}\}$ the corresponding tracks or clusters are combined to a single object; the procedure is repeated until all tracks or clusters are assigned to jets. The algorithm is suited to handle overlapping jets, facilitates the separation between beam remnants and hard scattering fragments and yields smaller higher order QCD and fragmentation corrections than e.g. the cone algorithm.

Jet cross sections are calculated by convoluting the matrix element of the specific hard scattering process with the pdfs of the target proton. Examples of LO hard scattering processes are boson-gluon-fusion and QCD-Compton scattering (fig. 1). The parton evolution requires the summation of $\ln Q^2$ - and $\ln 1/x$ -terms, which is equivalent to a summing of ladder graphs pictured in fig. 1. In the DGLAP-approach [2] only leading powers of $\ln Q^2$ -terms are summed implying a strongly ordered increase of the virtuality of the exchanged partons towards the hard scattering. At small x where at HERA Q^2 is constrained to not too large values, the BFKL treatment of the parton evolution [3] is more appropriate, which resums $\ln 1/x$ -terms to all orders but retains the full Q^2 dependence; the parton chain is strongly ordered in x i.e. $x \ll x_g \ll \dots \ll 1$, implying k_T -unintegrated (gluon) pdfs and off-shell matrix elements for the hard scattering process. In the CCFM ansatz [4]

colour coherence in the evolution ladder is taken into account imposing an angular-ordering of the gluon emission with the maximum angle determined by the hard scattering subprocess; the cross section factorizes into pdfs unintegrated both in k_T and the gluon angle and an off-shell matrix element. At asymptotic energies CCFM evolution approaches BFKL at small x and DGLAP at large x and Q^2 .

While at high Q^2 the virtual photon behaves as a pointlike particle, at low Q^2 and in particular in photoproduction with $Q^2 = 0$, its hadronic structure has to be taken into account. The momentum transfer from the scattered electron to the parton cascade then takes place via a parton of the "resolved photon", which itself may evolve in a parton cascade towards the hard scattering process. Such resolved processes contribute a background to hard scattering processes but also can serve as a tool to investigate the photon structure function.

The response of the detectors to jet events is studied with Monte Carlo generated events, which are based on the measured pdfs of the proton and photon and on simulations of the fragmentation and hadronization of the partons. In RAPGAP the QCD matrix element is calculated in LO with NLO corrections evaluated by perturbative generation of parton showers; the hadronization of the partons is performed via JETSET, which is based on the Lund-string model. In ARIADNE, the parton cascade is generated using the colour-dipole-model (CDM) while in CASCADE it is calculated via CCFM evolution.

2 Jets in DIS

The inclusive jet cross section σ_j results from the convolution of the measured pdfs of the proton $f_a(x_a, \mu_F)$ with the perturbatively calculated hard partonic cross section $d\sigma_a(x_a, \alpha_s, \mu_R, \mu_F)$,

$$\sigma_j = \sum_a \int dx f_a(x, \mu_F^2) d\sigma_a(x, \alpha_s, \mu_R^2, \mu_F^2) (1 + \delta_{\text{hadr}})$$

where the sum is to be taken over all partons a of the proton; σ_j has to be folded with the bremsstrahlung spectrum. μ_R is the renormalization scale and μ_F the factorization scale. $(1 + \delta_{\text{hadr}})$ represents the nonperturbative correction accounting for the hadronization of the partons; it is estimated from MC generators.

(i) Single jet cross sections have been measured by H1 and ZEUS in the Breit frame using the k_T -cluster algorithm. The kinematical parameters for the H1 data [5] are $150 < Q^2 < 5000 \text{ GeV}^2$, $7 < E_T < 50 \text{ GeV}$, $-1 < \eta_{\text{lab}} < 2.5$, while for the ZEUS data [6] they are $Q^2 > 125 \text{ GeV}^2$, $E_T > 8 \text{ GeV}$, $-2 < \eta_{\text{lab}} < 1.8$. The good agreement of both measurements with NLO QCD calculations (DISENT) at high Q^2 values (fig. 2) has enabled precision determinations of α_s and its scale dependence from these data (see Sect. 5).

The ZEUS data have been used to study the azimuthal distribution of jets in the Breit frame [7]. The measured ϕ -distribution agrees well with the NLO QCD predictions from DISENT with either $\mu_R = E_T$ or Q , providing an independent test of QCD.

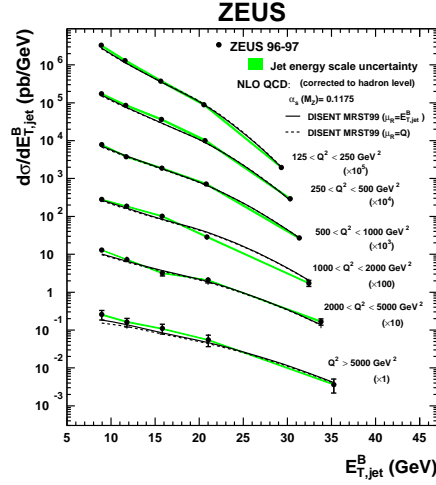


Figure 2: Inclusive jet cross section in DIS in the Breit system (fig. from [6])

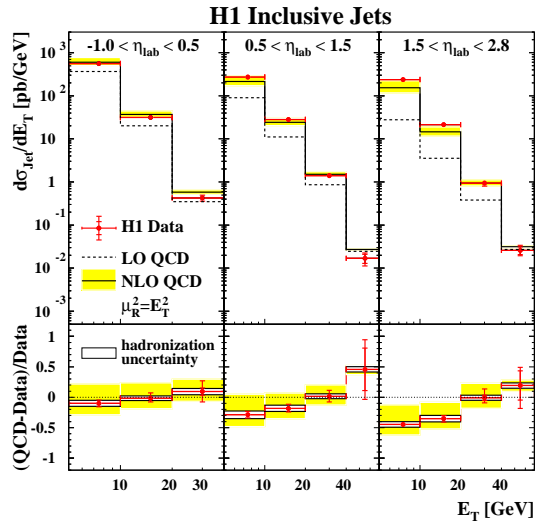


Figure 3: Inclusive jet cross section in DIS in the Breit system integrated over $5 < Q^2 < 100 \text{ GeV}^2$ and $0.2 < \eta_{\text{lab}} < 0.6$, NLO QCD: DISENT without hadronization correction; shaded band: change of renorm. scale by 1/2 and 2 (fig. from [18])

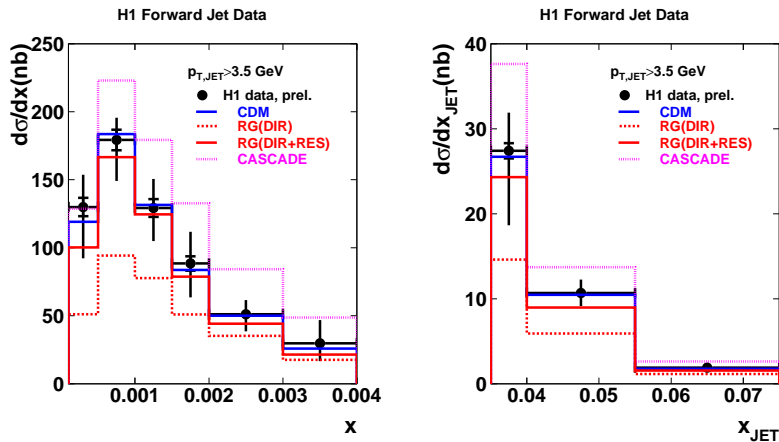


Figure 4: Inclusive jet cross section in DIS in the forward direction i.e. $7^\circ < \theta_{j\text{lab}} < 20^\circ$; CDM: Color-Dipole-Model; RG: RAPGAP; CASCADE: CCFM; (prelim. data, from [9])

H1 has extended the inclusive jet measurements [8] to low Q^2 values of $5 < Q^2 < 100 \text{ GeV}^2$, $-1 < \eta_{\text{lab}} < 2.8$, for $E_T > 5 \text{ GeV}$ and $0.2 < y < 0.7$. The good agreement of the differential cross section in E_T with NLO QCD (setting $\mu_R = E_T$) in the backward and central region worsens towards the forward direction i.e. $\eta_{\text{lab}} > 1.5$ and for $E_T < 20 \text{ GeV}$ (fig. 3). In this region, NLO corrections are large and theoretical uncertainties due to the uncertainty in the renormalization scale are larger than the experimental errors. Further studies have shown the discrepancies to NLO QCD to develop at $Q^2 < 20 \text{ GeV}^2$.

(ii) Data for inclusive jet production near the forward direction i.e. $7^\circ < \theta_{j\text{lab}} < 20^\circ$ have been taken by H1 [9] for $0.5 < Q^2/E_T^2 < 2$. The jet analysis using the k_T -cluster algorithm has been performed in the lab frame with cuts corresponding to $5 < Q^2 < 75 \text{ GeV}^2$ and $0.1 < y < 0.7$. In fig. 4 the data are compared with different QCD models. Reasonable agreement with DGLAP is achieved only if resolved photon processes are included, but also the colour dipole model describes the data reasonably well.

A process related to forward jet production is forward π^0 -production, which has been studied by H1 [10]; here the forward parton is tagged by a single energetic fragmentation product i.e. the π^0 . While in principle smaller angles than in jet production can be reached, the cross sections are lower and the hadronization uncertainties are higher. The data can be described by DGLAP models only after including resolved photon processes, but also BFKL models provide a reasonable description of the data.

(iii) LO contributions to dijet production are the QCD-Compton effect (QCDC) and boson gluon fusion (BGF) (see fig. 1). In the high Q^2 region where QCDC is dominating and the pdfs are well constrained by fits to F_2 data, dijet measurements using α_s as input can serve to test pQCD; alternatively, by comparing the data with pQCD, α_s (and its running) can be determined. At low Q^2 , where the cross section is dominated by BGF, the comparison of data with assumptions on the pdfs can constrain the gluon density distribution.

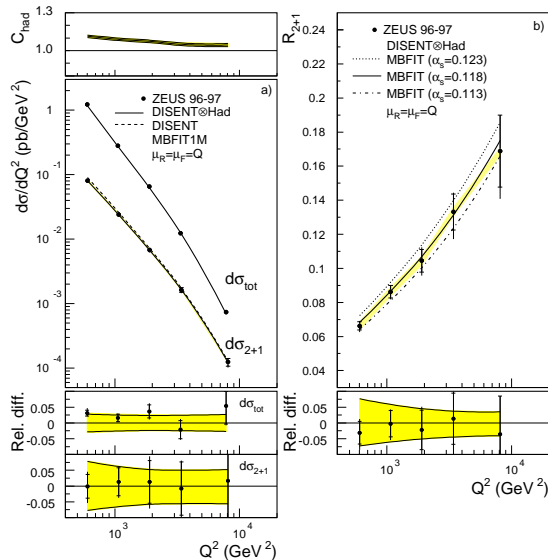


Figure 5: Inclusive jet ($d\sigma_{tot}$) and dijet ($d\sigma_{2+1}$) cross sections with dijet fraction R_{2+1} in DIS; shaded band: uncertainty in absolute energy scale of jets (fig. from [11])

Dijet data have been taken by H1 [1] and ZEUS [11] in similar kinematical regions and analyzed by similar methods. Asymmetric cuts have been applied in E_T in order to avoid infrared sensitive regions of the phase space. At not too low Q^2 and E_T i.e. $Q^2 > 10 \text{ GeV}^2$ and $E_T > 5 \text{ GeV}$, the data are reproduced (fig. 5) within 10% by NLO QCD (DISENT). For the α_s analysis of these data see Sect. 5.

Recent dijet-data from H1 [12] in the low- x region i.e. $10^{-4} < x < 10^{-2}$ for $10 < Q^2 < 100 \text{ GeV}^2$ agree within errors with DGLAP based NLO QCD predictions for inclusive cross sections. Serious disagreement is observed, however, in the ratio S of the number of dijet events with azimuthal separation $\phi < 2\pi/3$ to the total number of dijet events. While the LO (DISENT) prediction is much too low, the agreement is improved except in the low- x and low- Q^2 region if a third hard jet is included in the NLO (NLOJET) calculation (fig. 6). A comparison with RAPGAP shows that the inclusion of resolved processes improves the agreement except in the very low- x and low- Q^2 region. From a comparison of the data with the CCFM based CASCADE MC a strong sensitivity to the assumptions on the unintegrated gluon distribution can be inferred, which may be used to constrain the gluon pdf. ARIADNE, which is based on CDM, describes the low- x and low- Q^2 region reasonably well, fails, however, at larger Q^2 values.

The jet studies in deep inelastic scattering have been extended to trijets [13], [14] as well as to subjets [15].

3 Jets in photoproduction

The description of photoproduction involves the convolution of the hard partonic scattering cross section with the pdfs of both the proton and the photon. In standard jet production i.e. jets from light quarks only, for the energy scale $\mu_R = \mu_F = \mu =$

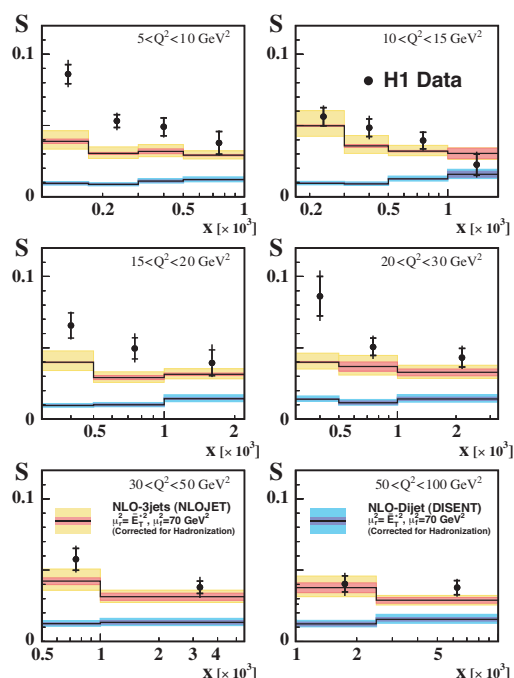


Figure 6: Ratio S of number of dijet events in DIS with azimuthal sep. $\phi < 2\pi/3$ between the two highest transverse momentum jets to the total number of dijet events compared with LO and NLO QCD predictions for dijet and trijet production; light shaded band: quadr. sum of hadroniz. error (dark shaded band) and renorm. error; (fig. from [12])

E_T is taken. Apart from the folding with the electron bremsstrahlung spectrum, the jet cross section is written as

$$\sigma_j = \sum_{a,b} \int \int dx_\gamma dx_p f_{pa}(x_p, \mu^2) f_{\gamma b}(x_\gamma, \mu^2) d\sigma_{ab}(x_p, x_\gamma, \alpha_s, \mu^2) (1 + \delta_{\text{hadr}}),$$

where the sum is to be taken over all partons a, b from the proton and photon.

(i) In single jet production a wider kinematic range is accessible than in dijet production, cross sections are higher and systematic errors due to the treatment of infrared unsafe regions are avoided; on the other hand, the reaction is less sensitive to details of the hard scattering process.

In recent measurements at $Q^2 < 1 \text{ GeV}^2$ of differential cross sections by ZEUS [16] and H1 [17] using the k_T -cluster algorithm in the lab frame, the kinematical range of $E_T > 5 \text{ GeV}$, $-1 < \eta_{\text{lab}} < 2.5$ and the photon-proton-cms energy W of $95 < W < 293 \text{ GeV}$ has been covered. While LO QCD calculations fail to reproduce the data in their normalization, good agreement is found with the corresponding NLO predictions (fig. 7, left). A subset of data taken by H1 at $Q^2 < 0.01 \text{ GeV}^2$ for $5 < E_T < 12 \text{ GeV}$ indicate an excess over predictions towards increasing η values. The precision of the experimental data and of the predictions is not yet sufficient to discriminate between different proton and photon pdfs. For the determination of $\alpha_s(M_Z)$ and its scale dependence from the data of [12] see Sect. 5.

In the ZEUS experiment [16] also the scaled invariant jet cross section $E_T^4 E d^3\sigma / dp_x dp_y dp_z$ has been measured as a function of the dimensionless variable

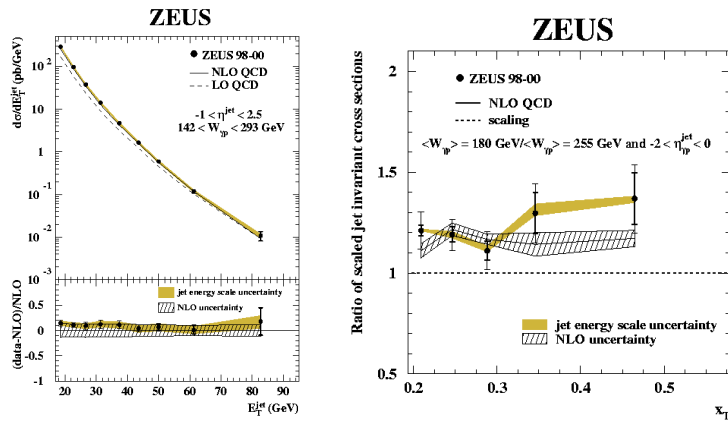


Figure 7: Inclusive jet production cross section in photoproduction. Ratio of scaled invariant cross sections (av. over $-2 < \eta_{\text{lab}} < 0$) for the two shown $\langle W_{\gamma p} \rangle$ compared with NLO QCD; (fig. from [16])

$x_T = 2E_T/W_{\gamma p}$ at $\langle W_{\gamma p} \rangle = 180$ and 255 GeV. The cross section ratio as function of x_T violates scaling as predicted from QCD (fig. 7, right).

(ii) The dijet photoproduction cross section is dependent on the dijet angle θ^* in the parton-parton-cms, which is sensitive to the matrix element of the hard scattering subprocess. Direct photon processes are dominated by BGF with the angular dependence of the spin 1/2-progator $\sim (1 - \cos \theta^*)^{-1}$ whereas in resolved processes gluon-exchange with the steeper angular dependence of the spin 1-progator $\sim (1 - \cos \theta^*)^{-2}$ is dominating. The dijet events can be enriched with direct or resolved processes by cutting on the fraction x_γ^{obs} of the photon-momentum transferred to the two jets of highest transverse energy, which is given by $x_\gamma^{\text{obs}} = (E_{T1}e^{-\eta_1} + E_{T2}e^{-\eta_2})/2yE_e$ with y the fractional electron energy carried by the photon in the p -rest frame.

Dijet photoproduction has been studied by ZEUS [18] and H1 [19] under similar kinematical conditions using the k_T -cluster algorithm. The differential cross sections in the dijet invariant mass, E_T and η agree well with NLO QCD expectations and in particular the measured dijet angular distributions (fig. 8) shows the expected difference for direct ($x_\gamma^{\text{obs}} > .75$) and resolved processes ($x_\gamma^{\text{obs}} < .75$). The sensitivity of the data to the parametrization of the photon-pdfs appears to be affected by the choice for the E_T -cuts (ZEUS: $E_{T1} > 14$ GeV, $E_{T2} > 11$ GeV; H1: $E_{T1} > 25$ GeV, $E_{T2} > 15$ GeV).

4 α_s -determinations

The good agreement of jet cross sections with QCD predictions has enabled determinations of α_s and its scale dependence.

The H1 inclusive jet cross sections [5] as a function of E_T have been fitted to the QCD prediction for four regions of Q^2 using the proton-pdfs and μ_R and μ_F as input. The resulting α_s has been shown to be stable against variations of the jet

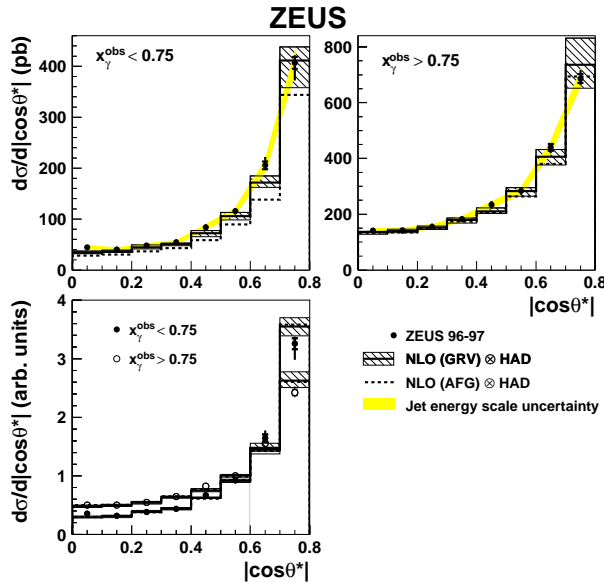


Figure 8: Inclusive dijet photoproduction as a function of the dijet angle θ^* in the parton-parton-cms for different cuts on the fractional photon momentum x_γ^{obs} transferred to the dijet system. Comparison with NLO QCD for different photon-pdfs; (fig. from [18])

algorithm. The combined fit to all Q^2 -data evolved to m_Z is shown in the summary fig. 9).

For the analysis of the ZEUS data [6] the following procedure has been applied: The cross sections $d\sigma/dA$ with $A = Q^2, E_T$ have been calculated in NLO QCD for the same pdf-set with three α_s -values. These calculations were used to parametrize the α_s -dependence of the binned cross sections $(d\sigma/dA)_i$ for each bin i according to $(d\sigma(\alpha_s)/dA)_i = C_{1i} \cdot \alpha_s^1 + C_{2i} \cdot \alpha_s^2$ with $\alpha_s = \alpha_s(M_Z)$. From a χ^2 -fit of this ansatz to the measured $d\sigma/dA$, α_s was obtained for the chosen regions of A . The best fit was obtained for $Q^2 > 500 \text{ GeV}^2$ (fig. 9). The same procedure has been applied to determine the scale dependence of α_s . With E_T as energy scale, the α_s dependence of $d\sigma/dE_T$ was parametrized in terms of $\alpha_s(\langle E_T \rangle)$ where $\langle E_T \rangle$ is the mean value of E_T in bin i . The result is shown in fig. 10.

The same method has been applied to other jet results from ZEUS i.e. the dijet fraction [12], subjet multiplicities ([15]) and jets from photoproduction [15]. A summary of the results is shown in figs. 9 and 10.

5 Summary

In the analysis of jet production in DIS and photoproduction at HERA the longitudinally invariant k_T -cluster algorithm in its inclusive version has become the standard jet finding algorithm.

In DIS, the inclusive jet cross sections at higher values of Q^2 and E_T are well described by NLO QCD; in this region higher order and hadronization corrections are small; this holds as well for photoproduction.

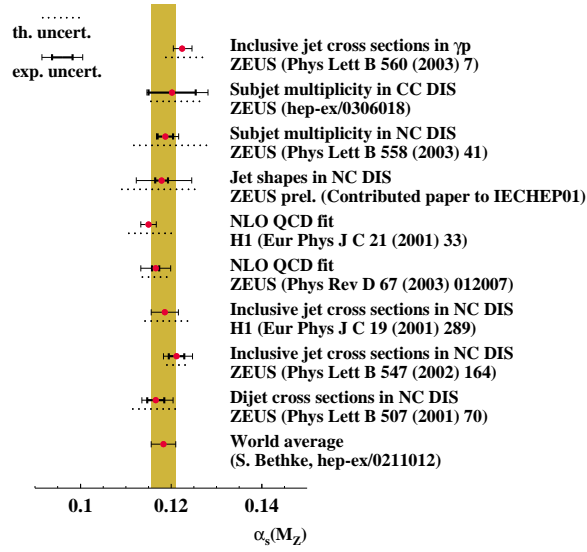


Figure 9: $\alpha_s(M_Z)$ from recent H1 and ZEUS measurements and the world average

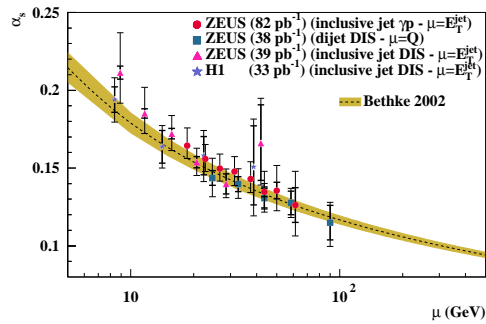


Figure 10: Scale dependence of α_s from recent H1 and ZEUS measurements and QCD predictions for $\alpha_s(M_Z) = 0.1183$ (world average)

In the forward region and/or at smaller Q^2 resp. x values, the situation is less satisfactory. DGLAP based calculations are expected to become less reliable in this region, the mentioned corrections are sizable and the hadronic structure of the photon i.e. resolved processes have to be taken into account. Calculations based on BFKL or CCFM evolution only partly show better agreement. An increase in experimental statistics and efforts to reduce the theoretical uncertainties are highly desirable for a better understanding of this challenging region.

The measurements of α_s and its running from jet data have yielded results which are of perhaps unexpected precision; they can well compete with other precision measurements e.g. from e^+e^- -annihilation and are in good agreement with the world average.

Acknowledgements I thank G. Grindhammer for valuable discussions and comments on the paper.

References

- [1] S.D. Ellis and D.E. Soper, Phys. Rev. D48, 3160 (1993) [hep-ph/9305266];
S. Catani et al., Nucl. Phys. B406, 187 (1993)
- [2] V. Gribov and L.N. Lipatov, Sov. J. Nucl. Phys. 15, 438, 675 (1972);
L.N. Lipatov, Sov. J. Nucl. Phys. 20, 94 (1975);
G. Altarelli and G. Parisi, Nucl. Phys. B126, 298 (1977);
Y.L. Dokshitzer, Sov. Phys. JETP 46, 641 (1977)
- [3] V.S. Fadin, E.A. Kuraev and L.N. Lipatov, Sov. Phys. JETP 44, 443(1976);
V.S. Fadin, E.A. Kuraev and L.N. Lipatov, Sov Phys. JETP 45, 199 (1977);
Y. Balitsky and L.N. Lipatov, Sov. J. Nucl. Phys. 28, 822 (1978)
- [4] M. Ciafolini, Nucl. Phys. B296, 49 (1988);
S. Catani, F. Fiorani and G. Marchesini, Phys. Lett. B234, 339 (1990);
S. Catani, F. Fiorani and G. Marchesini, Nucl. Phys. B336, 18 (1990);
G. Marchesini, Nucl. Phys. B445, 49 (1995) [hep-ph/9412327]
- [5] C. Adloff et al., Europ. Phys. J. C19, 289 (2001) [DESY 00-145;
hep-ex/0010054]
- [6] S. Chekanov et al., Physics Letters B547, 164 (2002) [DESY 02-112;
hep-ex/0208037]
- [7] S. Chekanov et al., Physics Letters B551, 226 (2003) [DESY 02-171;
hep-ex/0210064]
- [8] C. Adloff et al., Physics Letters B542, 193 (2002), [DESY 02-079;
hep-ex/0206029]
- [9] J. Jung: H1 Collaboration, ICHEP 02, Amsterdam (2002)
- [10] L. Goerlich: H1 Collaboration, DIS 2003, St. Petersburg (2003)
- [11] J. Breitweg et al., Physics Letters B507, 70 (2001) [DESY 01-018;
hep-ex/0102042];
S. Chekanov et al., Europ. Phys. J. C23, 13 (2002) [DESY 01-127;
hep-ex/0109029]

- [12] A. Aktas et al.: H1-collaboration DESY 03-160; hep-ex/0310019
- [13] C. Adloff et al., Physics Letters B515, 17 (2001) [DESY 01-073; hep-ex/0106078]
- [14] N. Krumnack: ZEUS Collaboration, DIS 2003, St. Petersburg (2003)
- [15] S. Chekanov et al., Physics Letters B558, 41 (2003) [DESY 02-217; hep-ex/0212030]
- [16] S. Chekanov et al., Physics Letters B560, 7 (2003) [DESY 02-228; hep-ex/0212064]
- [17] C. Adloff al., submitted to Europ. Phys. J. C [DESY 02-225; hep-ex/0302034]
- [18] S. Chekanov et al., Europ. Phys. J. C23, 615 (2002) [DESY 01-220; hep-ex/0112029]
- [19] C. Adloff et al., Europ. Phys. J. C25, 13 (2002) [DESY 01-225; hep-ex/0201006]